

# Validation of satellite cloud effective radius using ORACLES data

Aydin, Onurhan

Johann Wolfgang Goethe University, Frankfurt am Main

Report of Remote Sensing and Climate Diagnostic (SoSe 2022)

2022-07-28

---

**Abstract:** Aerosols are important components of the atmosphere, and satellite measurements are essential for observing how they interact with radiation and clouds. It is helpful to understand how they affect both regional and global climate in order for modeling with better forecast. Observations with a 15-minute temporal resolution are provided in datasets from geostationary satellite instruments like the Spinning Enhanced Visible and Infrared Imager (SEVIRI), which are crucial data sources to assess and eventually better understand cloud processes, e.g. the interaction of aerosols with clouds. In this study, we compare data from SEVIRI cloud effective radius based on two different channel combinations (0.6 and 1.6; 0.6 and 3.9) from CLAAS-3 (CLoud property dAtAset using SEVIRI, Edition 3) to aircraft measurement data from the ObseRvations of Aerosols above Clouds and their IntEractionS (ORACLES). The evaluation findings reveal reasonable agreement of the satellite data with the aircraft measurements. Major differences weren't discovered.

---

## 1 Introduction

One of the critical geographic regions for comprehending the connections between the Earth's climate, weather, and pollution is the southeastern (SE) Atlantic and the west coast of southern Africa. A stratocumulus cloud deck, strong large-scale subsidence, and the anticyclonic circulation of the semi-permanent southern Atlantic sea level pressure high are its defining features. Nearly a third of the biomass burning (BB) aerosol particles that are produced on Earth come from Southern Africa, which is seen in fig. 1, yet little is known about how they affect local and global weather and climate. The aerosols interact with clouds. Microphysical effects and modifications to aerosol-induced solar heating are examples of these interactions. The global depiction of these aerosol-cloud interaction processes in climate models is one of the great challenges for model projections of the future climate, as highlighted in the most recent IPCC report [1]. The primary objectives of the ORACLES campaign are to first ascertain the influence of African BB aerosol on cloud

properties and the radiation balance over the South Atlantic. It is performed by using cutting-edge in-situ and remote sensing instruments to produce data sets that can also be used to verify and improve current and future observation methods. Furthermore, ORACLES aims at acquiring process-level understanding of aerosol-cloud-radiation interactions and resulting cloud adjustments that can be applied in global models. SEVIRI measurements serve as the basis for CLAAS-3. SEVIRI is a passive visible and infrared imager that is mounted on the Meteosat Second Generation (MSG) satellites 1 through 4 also known as Meteosat-8 to 11. These satellites are geostationary and can provide a 15-minute SEVIRI imaging repeat cycle due to their rotation [2]. Approximately 12 minutes are spent by SEVIRI scanning the Earth's surface from south to north; the remaining five minutes are spent processing and transferring the data [3]. The size and shape of the footprint of one particular satellite pixel are not uniform across the surface because of the scan geometry. According to fig. 2, spatial resolution is highest near the sub-satellite point at 0° latitude and 0° longitude coordinates, but the resolution decreases with distance from these points due to the increasing satellite zenith angle.

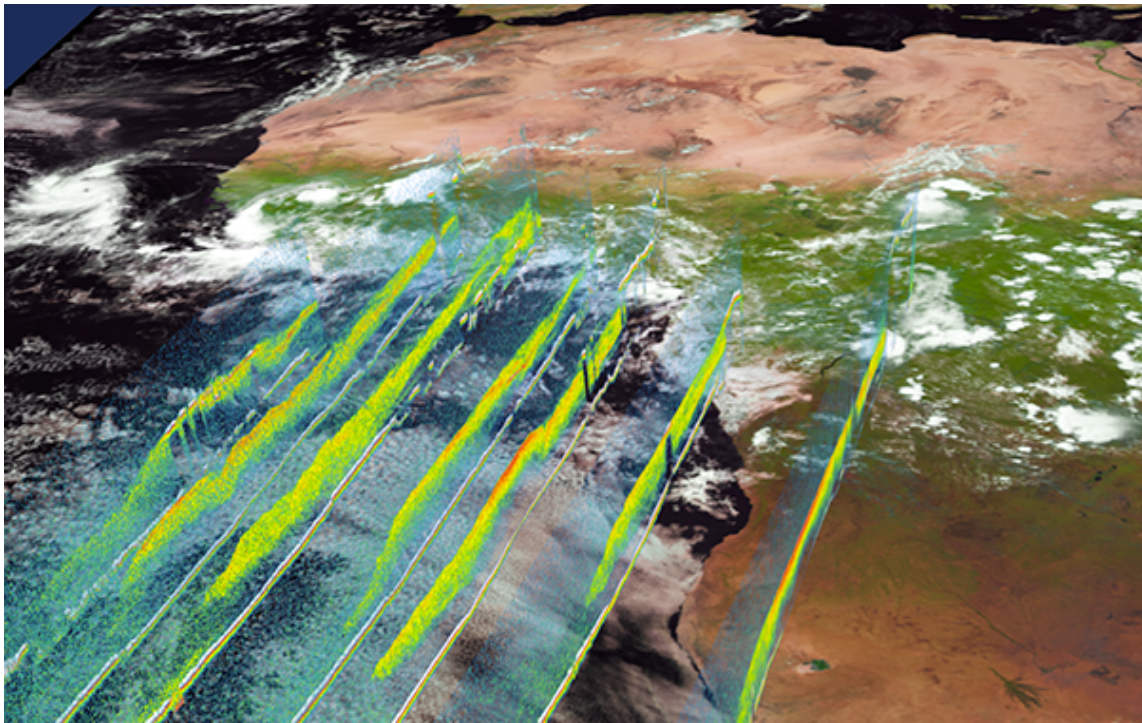


Figure 1: Aerosol BB's widespread transportation from the Region of interest  
(<https://espo.nasa.gov/oracles/>)

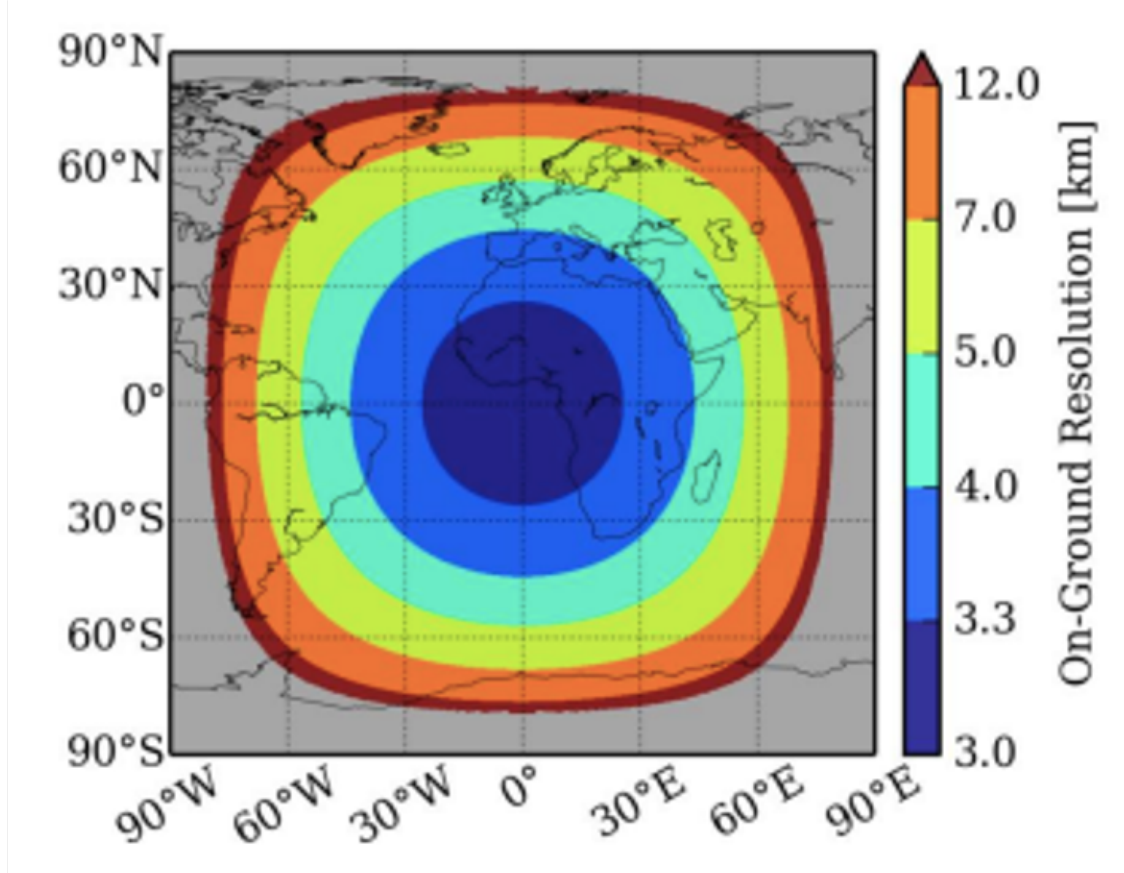


Figure 2: Temporal and spatial resolutions of SEVIRI

## 2 Data Sets

### 2.1 SEVIRI

Onboard the geostationary METEOSAT second generation satellites, the Spinning Enhanced Visible and Infrared Imager (SEVIRI) delivers observations with a temporal resolution of 15 minutes and measures in the visible and infrared. SEVIRI is able to scan Africa, Europe, Asia, and as well as South America. It has 11 visible and infrared channels with a spatial resolution of 3 km. Additionally, resolutions of the High Resolution Visible (HRV) channel is 1 km. Cloud measurements are obtained from CLAAS-3 dataset ([https://doi.org/10.5676/EUM\\_SAF\\_CM/CLAAS/V003](https://doi.org/10.5676/EUM_SAF_CM/CLAAS/V003)) for which SEVIRI measurements were the input. To reduce potential errors, the data set excludes measurements with a solar zenith and viewing zenith angles larger than 84° [4] for variables that need solar measurements. There are numerous cloud parameters in the CLAAS-3 dataset. These parameters are Liquid Water Path (LWP), Ice Water Path (IWP), Cloud Top Level (CTO), Cloud Phase (CPH), and Fractional Cloud Cover (CFC). For all cloud parameters, the CLAAS-3 dataset includes a number of algorithm improvements compared to its precursor version CLAAS-2 [8]. Through its frequent observations, SEVIRI allows for providing precise estimates of daily and monthly averages for all properties that have a high temporal

variability. Additionally, the measured quantities' diurnal cycle may be accurately characterized, adding more clarity to the processes of cloud formation and atmospheric motion. With its capacity to distinguish between diurnal cycles, it can be viewed as supplementary data to long-term global cloud property datasets like CLARA, (Cloud cci), PATMOS-X, MODIS, and ISCCP, offering corresponding uncertainty measures or even correction for datasets purely based on polar orbiters [3].

In the project, one of the challenging tasks was to convert the projection information given in the CLAAS-2 data to geographical coordinates in order to process the raw data and visualise the data in a map. A sample visualisation of the CLAAS-3 cloud effective radius (CRE) is shown in fig. 3. X-axis displays longitude and Y-axis does latitudes. CRE values in this scene range from below 10 to 30  $\mu\text{m}$ , with some cloud edge pixel showing exceptionally high values of up to or even beyond 60  $\mu\text{m}$ . The areas with the most clouds are over Liberia and Cote d'Ivoire, although clouds with the largest radius are over southwest of the coast in Cote d'Ivoire. The year-round southeasterly trade winds may be the main cause of this convergence process. Clear-sky pixels are shown as white areas in this figure.

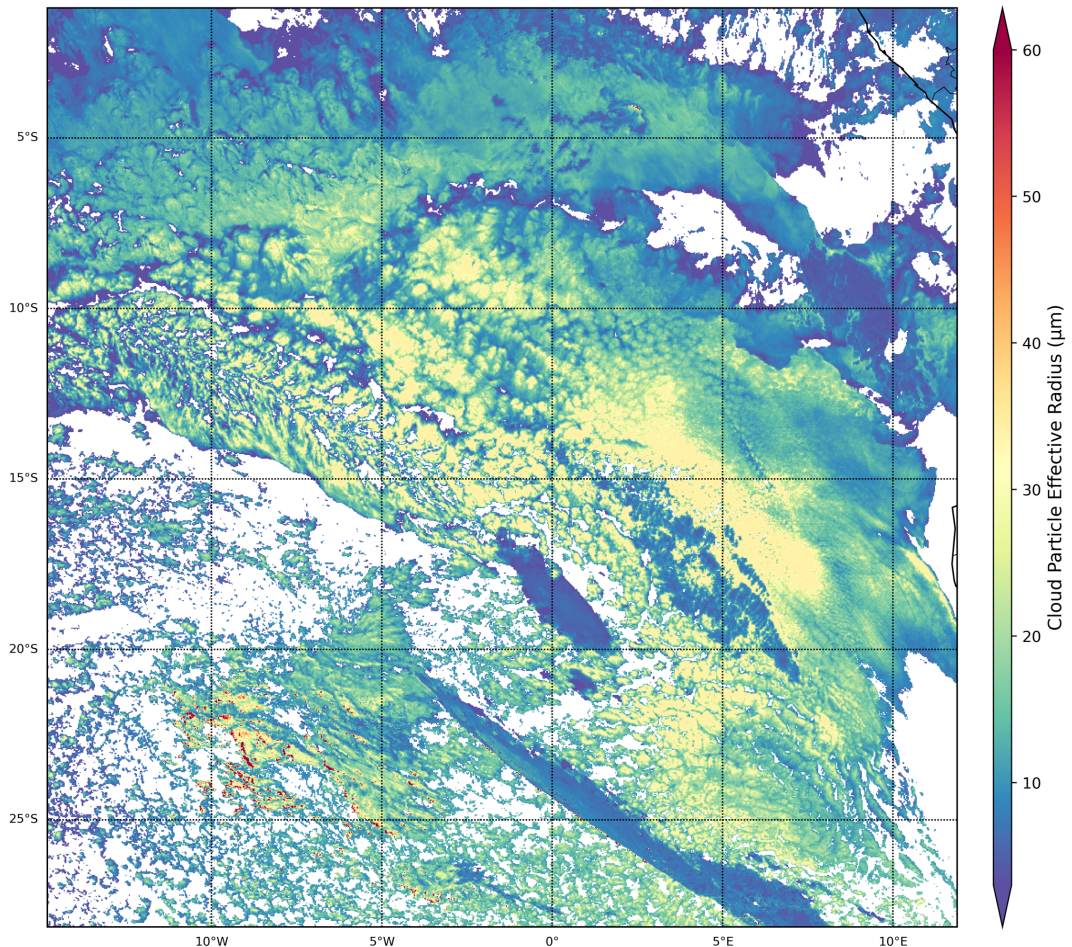


Figure 3: An illustration from SEVIRI satellite at 08.30 UTC on 2 September, 2016

## 2.1 ORACLES

To learn more about how biomass burning (BB) aerosol transport to the SE Atlantic Ocean affects climate, the ObseRvations of Aerosols above CLOUDs and their intEractiOnS (ORACLES) project deployed research aircraft flies for three months to the SE Atlantic Ocean. The objective was to comprehend how the transport of southern African BB aerosol over the Atlantic Ocean affect the climate. Therefore, it is vital to examine the meteorological features and how they deviate from the climatological mean at various temporal and spatial scales. The data format for measurement taken by aircraft using data from September 2, 4, and 10 was 'ict' (ICARTT - International Consortium for Atmospheric Research on Transport and Trans- formation). The aircraft used in the study is P-3 Orion (N426NA) research aircraft for the NASA Airborne Science Program. Since 1991, the P-3 has been used to support several scientific investigations, including those in the fields of ecology, meteorology, atmospheric chemistry, cryospheric research, oceanography, soil science, biology, and satellite calibration and validation [1]. In addition to this, the device utilised to measure CER, which is used in this study, is called 4STAR (Spectrometers for Sky- Scanning Sun-Tracking Atmospheric Research) airborne sun-sky spectrophotometer that collects and remotely senses column-integrated and vertically resolved data on aerosols, clouds, and trace gases. It measures direct solar beam transmittance and narrow field of view sky radiance. The figure 4 illustrates measurement points in the core campaign regions. Although the aircraft has performed flights in August, September and October in 2016, 2017 and 2018, only measurements from 2,4, and 10 of September 2016 will be analysed in this report. As previously mentioned, the region where the aircraft has flown is characterized by frequent and important interactions between aerosols, radiation and clouds.

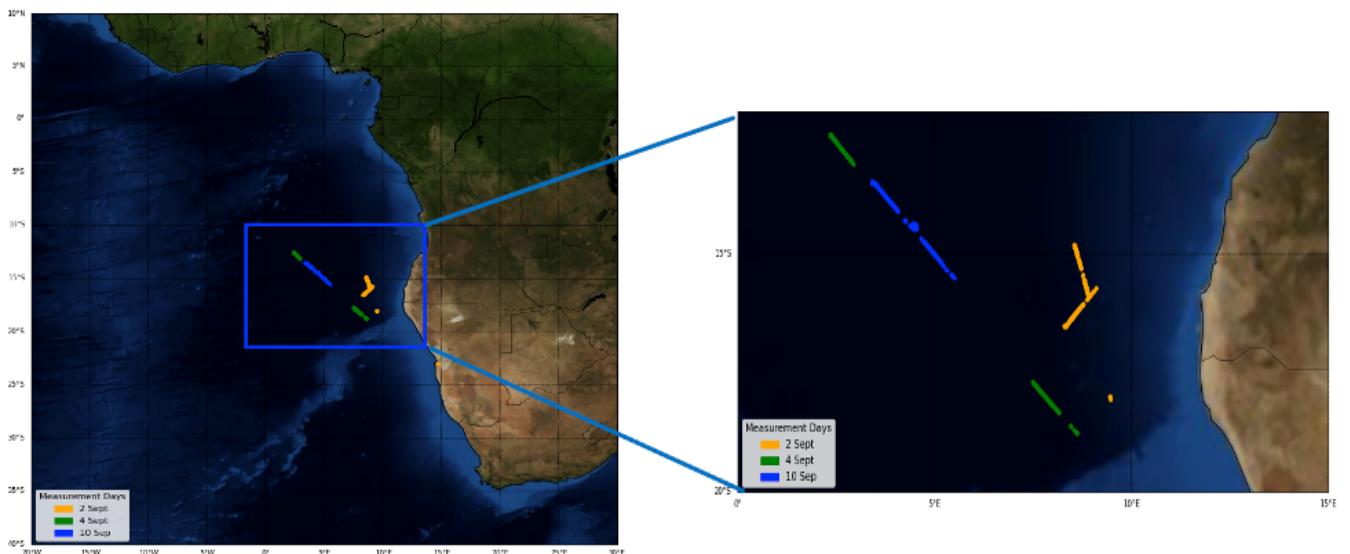


Figure 4: Points of aircraft measurements for 2, 4, and 10 of September

As can be seen in fig. 5, all aircraft data were converted to 'csv' format for Python manipulation. The time column, which represented the total duration (s) of time after the aircraft's takeoff, was also changed to UTC time at the same time. The latitude and longitude dimensions of the satellite data were then in projection coordinate, but the conversion was also done to the appropriate geographical coordinate format. The index of the measurement point closest to the satellite data coordinates is already calculated for each aircraft measurement point. The information made it simple to match the locations that were near to one another. After being combined, the satellite data and aircraft measurement data are now ready further analysis and visualization.

```
days=["02", "04", "10"]

for d in days:
    dn=pnc.pncopen(path+"4star/"+"4STAR-CLD_P3_201609"+d+"_R2.ict", format="ffil001")
    dn.save(path+"4star/"+"day"+d+".nc")
    ds=xr.open_dataset(path+"4star/"+"day"+d+".nc")
    df=ds.to_dataframe()
    df = df.apply (pd.to_numeric, errors="coerce")
    df['time'] = df['Start_UTC'].apply(lambda x: str(datetime.timedelta(seconds=x)))
    df["time"] = pd.to_datetime(df["time"])
    df["time"] = pd.to_datetime(df["time"]).dt.strftime('%H:%M:%S')
    df["year"] = 2016
    df["month"] = 9
    df["day"] = int(d)
    df["hour"] = pd.DatetimeIndex(df.time).hour
    df["min"] = pd.DatetimeIndex(df.time).minute
    df.to_csv(path+"4star/"+"day"+d+".csv")
    os.remove(path+"4star/"+"day"+d+".nc")
```

Figure 5: Snippet of implemented Python code for conversion of data format for 2, 4, and 10 September

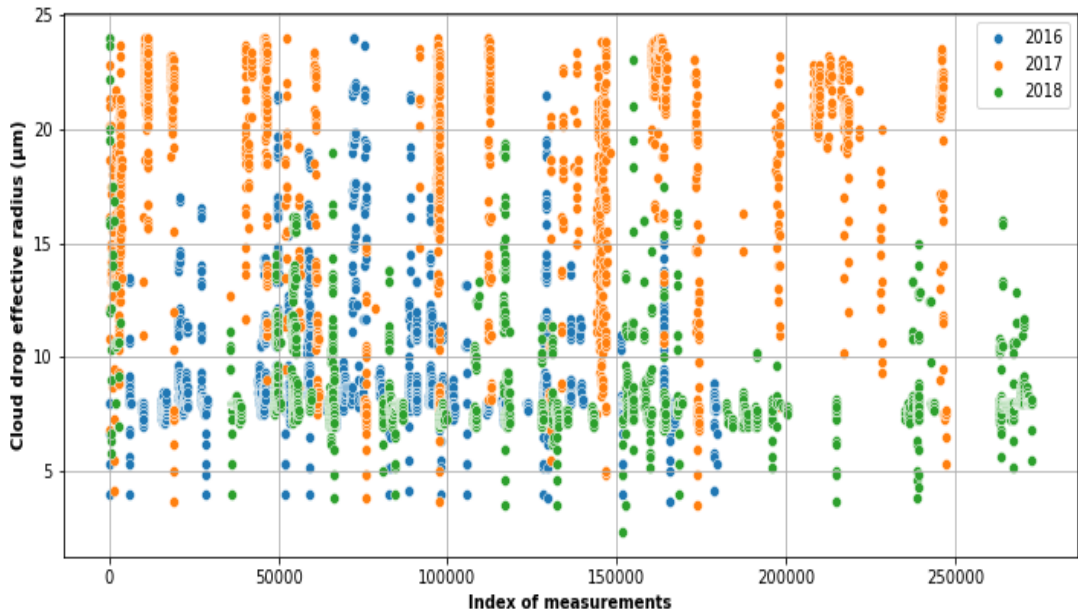


Figure 6: All data points of aircraft measurements in 2016, 2017, and 2018.

Figure 6 displays each measurement taken during the entire ORACLES campaign after removing invalid data points. The dots in each color stand for the years 2016, 2017, and 2018, respectively. The X-axis of the graph represents the measurement data index, and the Y-axis shows the effective radius of the clouds. According to observation, 2017 had higher values than 2018, which is the year with the lowest measurement values. Additionally, the range of the values is wider in 2017 than it was previously. 2018 measurements have a lower average than past years with many measurements being between 5 to 10 millimeters. Even though the aircraft data was colocated to the closest satellite pixel, a remaining mismatch in exact location and in spatial representativeness are a non-negligible source impact the results. Furthermore, the aircraft flew through the cloud, despite the fact that satellites can only see the tops of clouds. This could lead to measurement bias between satellites and aircraft. For future studies this could be revised as well as further information used, e.g. the flight altitude of the aircraft.

### 3 Results and Discussion

The results of the evaluation of the satellite data are presented and discussed in this section. Figures 7, 8 and 9 show the comparisons for September 2, 4, and 10, 2016. The Y-axis displays cloud effective radius in  $\mu\text{m}$ , while the X-axis shows time. The blue highlighted dots depict aircraft data, the orange dots show satellite cre variables, and the green dots illustrate satellite cre16 variables. Fig. 7 primarily shows three clusters. All measurements are closest to one another in the first cluster which is the most uniform set. But compared to other measurements, satellite-cre has more outliers. In the second cluster, aircraft measurement has a tendency to be greater, and this tendency is very apparent in the third cluster. Fig. 8 displays the measurements taken on September 4 from 9:00 AM to 11:00 AM UTC. There are primarily 2 data clusters in this graph. Since the range of satellite-cre is greater than that of other measurements, its values are more spread. The agreement is better 2 hours later, although the aircraft data are clearly higher than cre16. The day with the most measurements (10 September) is depicted in fig. 9. Measurements on that day were taken between 10:00 and 13:00 UTC. Four data clusters are visible. For the first cluster in the figure, the overestimation of satellite-cre measurement is clearly visible. Figure 10 shows all valid data points from the three selected days in September 2016 in a scatter plot. The X-axis displays the REF aircraft measurements, and the Y-axis displays the satellite data. Satellite-cre measurements are represented by yellow dots, and a regression line is represented by a yellow line. The green dots and line are for satellite-cre16 and represent, represent the regression line and data, respectively. Additionally, there are statistical parameters like bias and standard deviation in the bottom right corner. The regression line indicates that satellite-cre16 data and aircraft data are more closely correlated. The graph demonstrates that the average satellite-cre value is higher than satellite-cre16. However, a higher average could come with certain disadvantage. For instance, the bias and standard deviation of the satellite-cre are also larger than those of the satellite-cre16. As a result, the satellite-cre includes more spread values.

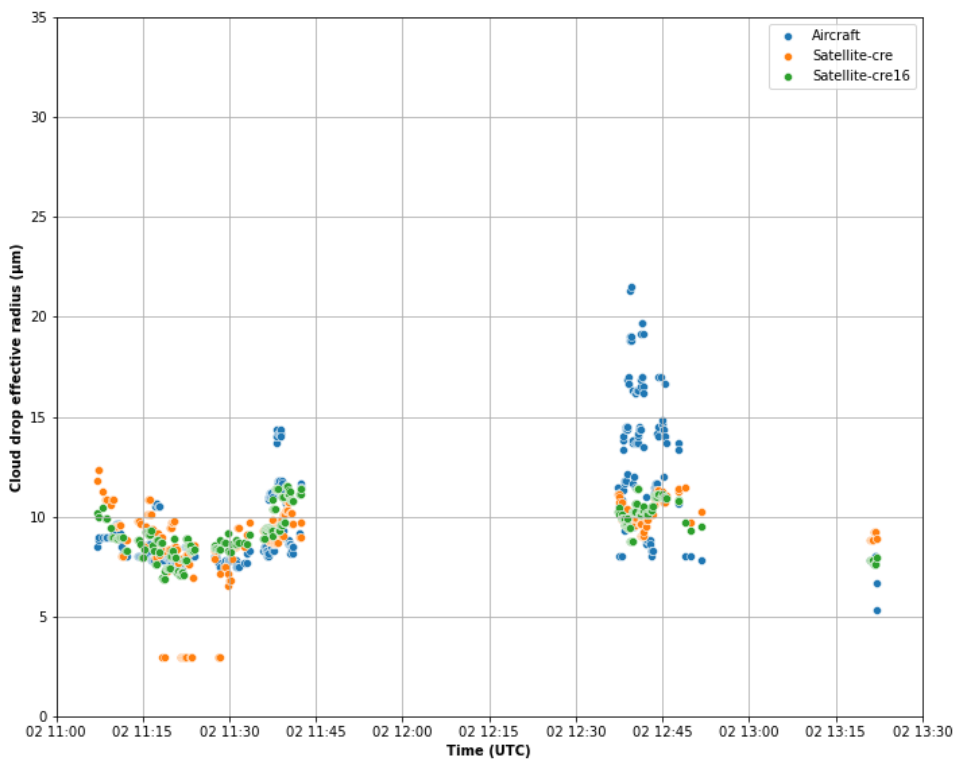


Figure 7: Aircraft and satellite measurements on 2 September

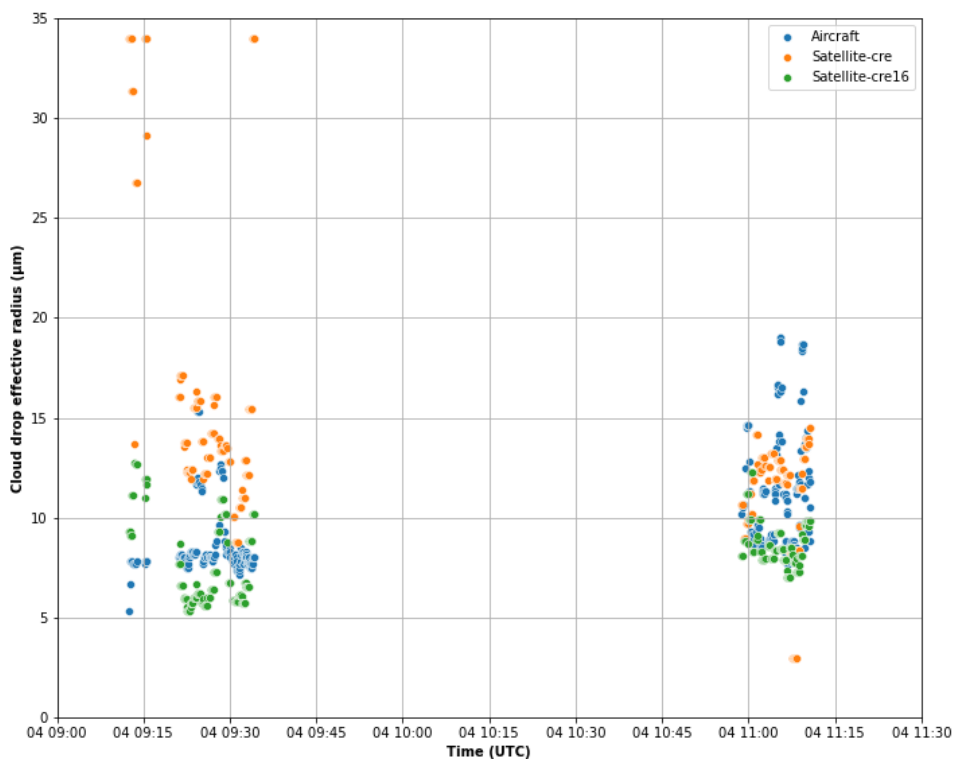


Figure 8: Aircraft and satellite measurements on 4 September

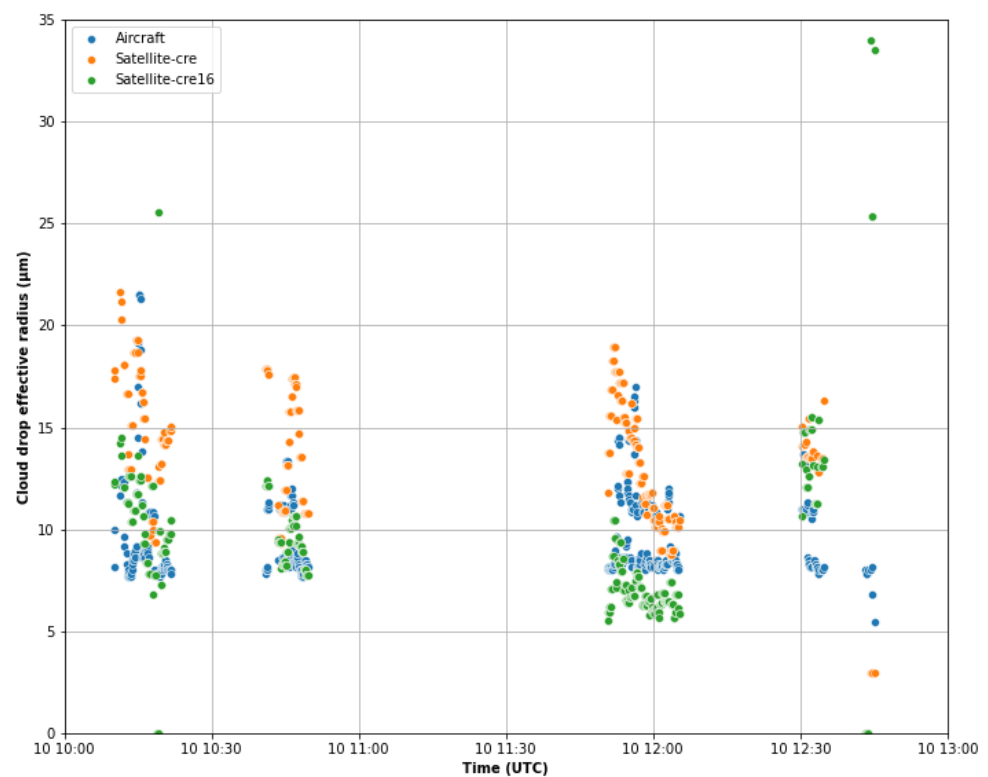


Figure 9: Aircraft and satellite measurements on 10 September

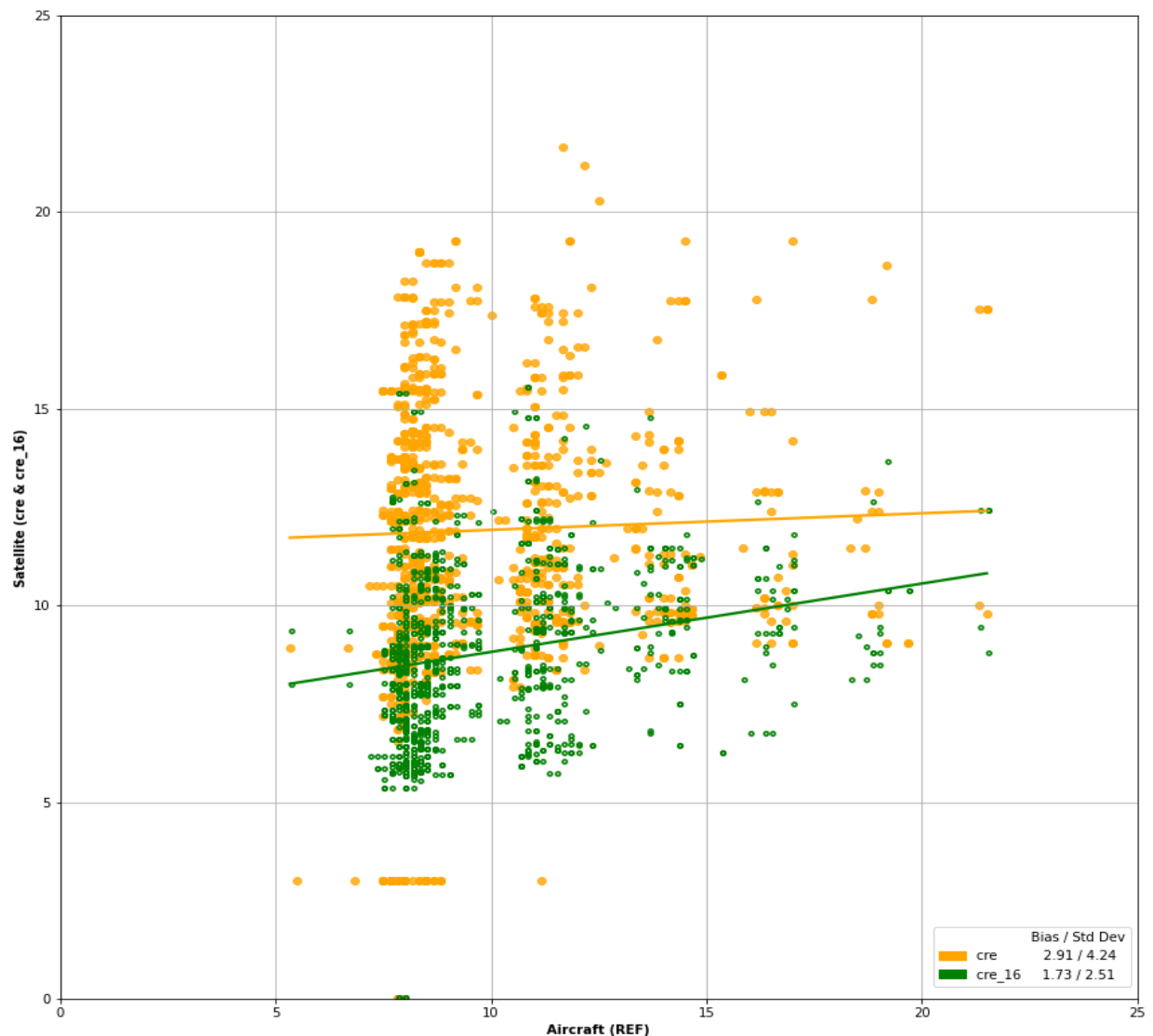


Figure 10: Scatter plot of all valid data from the three selected days in September 2016.

## 4 Summary and Conclusion

In this study, satellite-retrieved cloud effective radius products were evaluated using aircraft measurement taken during the ORACLES campaign held in the South-East Atlantic in 2016, 2017 and 2018. The satellite data was taken from the latest CLAAS dataset version (CLAAS-3), which is based on SEVIRI measurements. CLAAS-3 cloud affective radius exists in two realizations as cre and cre16. Overall, the results showed a reasonable agreement of the satellite data with the aircraft reference measurements. Standard deviations were 4.24 and 2.51  $\mu\text{m}$  for cre and cre16, respectively, while the biases were 2.91 dn 1.73  $\mu\text{m}$ . The findings provided here support the validity of CLAAS-3 data. Thus, CLAAS-3 can be regarded as a useful data source for research on cloud effective radius which is a key cloud property with respect to investigating aerosol-cloud interactions, generally but also in particular in the

stratocumulus region covered by the ORACLES campaign. More generally speaking, the CLAAS-3 record, with its many features of which the higher temporal and spatial coverage is one of the key elements, seems well suited for cloud processes.

## References

- [1] ORACLES. <https://espo.nasa.gov/oracles/> (Accessed July 19, 2022).
- [2] Meirink, J. F., Stengel, M., Benas, N., Solodovnik, I., Hakansson, N., and Karlsson, K., G.: Validation Report – SEVIRI cloud products, SAF/CM/DWD/PUM/SEV/CLD Issue 3, Rev. 3.0, Tech. rep., EUMETSAT Satellite Application Facility on Climate Monitoring, 2022.
- [3] Stengel, M., Kniffka, A., Meirink, J. F., Lockhoff, M., Tan, J. and Hollmann, R.: CLAAS: the CM SAF cloud property data set using SEVIRI, *Atmos. Chem. Phys.*, 14(8), 4297–4311, doi:10.5194/acp-14-4297-2014, 2014.
- [4] Coopman, Q., Hoose, C., Stengel, M. (2021). Analyzing the thermodynamic phase partitioning of mixed phase clouds over the Southern Ocean using passive satellite observations. *Geophysical Research Letters*, 48, e2021GL093225. <https://doi.org/10.1029/2021GL093225>
- [5] Taylor, S., Stier, P., White, B., Finkensieper, S., and Stengel, M.: Evaluating the diurnal cycle in cloud top temperature from SEVIRI, *Atmos. Chem. Phys.*, 17, 7035–7053, <https://doi.org/10.5194/acp-17-7035-2017>, 2017.
- [6] Bruno, O., Hoose, C., Storelvmo, T., Coopman, Q., Stengel, M. (2021). Exploring the cloud top phase partitioning in different cloud types using active and passive satellite sensors. *Geophysical Research Letters*, 48, e2020GL089863. <https://doi.org/10.1029/2020GL089863>
- [7] Benas, N., Finkensieper, S., Stengel, M., van Zadelhoff, G.-J., Hanschmann, T., Hollmann, R., and Meirink, J. F.: The MSG-SEVIRI-based cloud property data record CLAAS-2, *Earth Syst. Sci. Data*, 9, 415–434, <https://doi.org/10.5194/essd-9-415-2017>, 2017.
- [8] Finkensieper, Stephan; Meirink, Jan-Fokke; van Zadelhoff, Gerd-Jan; Hanschmann, Timo; Benas, Nikolaos; Stengel, Martin; Fuchs, Petra; Hollmann, Rainer; Werscheck, Martin (2016): CLAAS-2: CM SAF Cloud property dAtAset using SEVIRI - Edition 2, Satellite Application Facility on Climate Monitoring,  
DOI:10.5676/EUM\_SAF\_CM/CLAAS/V002, [https://doi.org/10.5676/EUM\\_SAF\\_CM/CLAAS/V002](https://doi.org/10.5676/EUM_SAF_CM/CLAAS/V002).